

Analysis of Sand Boiling Failure in Deep Excavations

Ignatius Tommy Pratama^(✉) and Chang-Yu Ou

National Taiwan University of Science and Technology, Taipei, Taiwan
tommyignatius@gmail.com

Abstract. Sand boiling is an issue of the stability of excavations in the sand under high groundwater level condition. Many approaches have been investigated in recent years to quantify the safety against sand boiling failure. Nonetheless, some conventional methods such as Terzaghi, Harza, Marsland, Harr, and the simplified one-dimensional techniques are still commonly used to analyze it due to their simplicity. Consequently, it may lead to a misinterpretation in predicting the failure condition because each method gives different values of the factor of safety. The objectives of this study are to predict the failure mechanism caused by groundwater flow and to perceive the factor of safety values in representing the safety against sand boiling. A series of the parametric study was carried out using the conventional method of flow net and numerical analysis to obtain the hydraulic gradient and the effective stresses in the excavation zone during groundwater flow. The numerical models involved 12 cases in a homogeneous dense sand and 11 cases in a homogenous loose sand with various excavation geometry. According to the analysed results, the excavation geometry and the soil density have some significant effects in governing the hydraulic gradient and the failure mechanism. It shows that the critical width of the soil prism is smaller than that is postulated by Terzaghi. Moreover, the most likely possible failure mechanism in loose sand is bulk heave of the soil prism, whereas the expulsion of the sand-water mixture on the excavation surface will be indicated in the dense sand cases.

Keywords: Sand boiling · Factor of safety · Failure mechanism · Excavation geometry · Sand density

1 Introduction

In the recent decades, the number of deep excavation projects for basements and tunnels has been widely increasing along with the growth of infrastructure needs in many urban areas. The limitation of open lands for further development is one of the reasons behind that trend. Nonetheless, deep excavation is a high-risk construction process to construct infrastructures because of the high-level uncertainty of soils and natural conditions. According to Ou (2006), in the design of deep excavation, there are several issues related to the stability of an excavation such as overall shear failure, upheaval failure, and sand boiling failure. Those concerns are relevant for layered cohesive and cohesionless soils cases, except sand boiling failure. It merely occurs in cohesionless soils under high groundwater level condition.

Sand boiling catastrophe in either excavation case or cofferdam case involves seepage flow in the mechanism failure. The movement of water inside the soil body can decrease or increase the effective stress of soil based on the direction of flow. It generates the unbalance forces along the sheet pile which leads to the disturbance of the equilibrium condition. Once the failure occurs, it becomes an unstoppable incidence because of the rapid occurrence. A proper analysis should be conveyed to estimate the safety of an excavation against sand boiling. Various conventional approaches such as Terzaghi (1922), Harza (1935), Marsland (1953), Harr (1962), and Ou (2006) methods have been studied. Those methods derived from either experimental models or mathematical approaches to express the safety against sand boiling failure in an excavation and cofferdam systems. Due to the development of advanced technology in computing some challenging and time-consuming mathematical formulas, numerical analysis becomes a promising and reliable approach to capturing and observing the behaviour of sand boiling failure. Nonetheless, the conventional methods are still widely used by engineers because of their simplicity.

The major issue related to the traditional approaches is the number of techniques in which it can offer a reasonable and reliable factor of safety and simulate well the real condition. Besides the number of methods, analysing the same case of excavation with different formulas will provide different values of the factor of safety. Different assumptions in each technique are suspected as one of the causes behind that phenomenon. Numerous researchers and geotechnical codes also have already suggested a different minimum standard of the factor of safety as a safe adequacy condition. As a matter of effect, it may lead to a misrepresentative information of the safety against sand boiling. Therefore, the objective of this research is to investigate several factors of safety formulas against sand boiling failure and other factors that govern its value in explaining the boiling failure phenomena by the two-dimensional numerical analysis and the conventional approaches. Moreover, the interpretation of effective stress distribution in the influence of groundwater flow to forecast the failure mechanism is also one of the interests of this work.

2 Philosophy of the Factor of Safety Against Sand Boiling

Terzaghi (1922) conducted model tests to perceive the mechanism of piping or sand boiling, and he found that the piping failure due to heave is initiated by the rise of the sand prism as shown in Fig. 1. The failure zone has a width, S about equal to the half of the wall penetration depth, $H_p/2$, and a depth of approximately equal to $H_{p,0}$ below excavation surface (i.e. $0 \leq H_{p,0} \leq H_p$). The piping failure condition attains when the effective weight of the prism, W' is less than or equal to the excess hydrostatic pressure, U_c which acts on the base of the prism. Simultaneously, the effective vertical stress at any section in the prism and horizontal stress on the sides of the prism are approximately nil. Furthermore, Terzaghi (1943) mentioned that the critical segment was represented by a depth of $H_{p,0}$ that the value nearly equals to H_p . Therefore, the factor of safety against piping is

where the water flows and leaves the soil mass by the shortest flow path. He defined the critical condition against sand boiling is attained when the ratio between i_c and i_e equals to one. Then, according to Harza (1935), the factor of safety against sand boiling can be expressed as

$$FS = i_c/i_e \tag{3}$$

The exit gradient, i_e of Harza (1935) definition can be obtained either from the conventional method of flow net or mathematical derivations. Harr (1962) investigated several circumstances of groundwater flow by the conformal mapping technique and proposed an analytical solution to estimate i_e for every particular groundwater flow case. According to Harr (1962), the critical exit point is located near the sheet pile or at point e as shown in Fig. 1. To make the equations to be more applicable for practice, Fig. 2 exhibits chart solutions to estimate the factor of safety against sand boiling in two distinct cases. In Fig. 2, the factor of safety trends were calculated by Harza (1935) formula with the i_c value equals unity, while the i_e values were estimated by Harr (1962) equation. If the i_c does not equal to one, multiply the $H_p/\Delta H_w$ ratio by the i_c value. Linear interpolation or logarithmic interpolation is allowable to be adopted in those charts. Harr (1962) also provided an exit gradient equation for a simple cofferdam case without impermeable layer beneath the toe of retaining wall as follows:

$$i_e = \frac{\Delta H_w}{H_p \pi} \tag{4}$$

Harr (1962) suggested that the minimum factor of safety value is greater than or equal to 4.0 to 5.0 to be considered adequate on the safety of excavation or dam against piping or boiling.

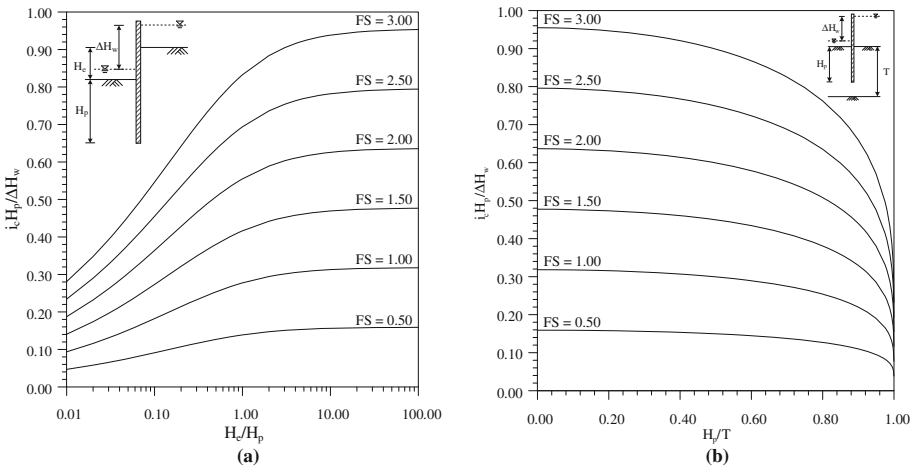


Fig. 2. Harr (1962) factor of safety against sand boiling

Harr (1962) implicitly showed that the geometry of a retaining system and the existence of impermeable layer affect the magnitude of exit gradient. His equations demonstrate that every equation is only applicable for a particular condition. To observe the influence of excavation geometry and the existence of impermeable layer, Fig. 3 depicts the reduction factors of impermeable layer, RF_{imp} and the reduction factor of excavation height, RF_{exc} . Those factors were obtained by comparing the exit gradient equations in which the exit gradient equations consider and do not consider the factors (i.e. the existence of impermeable layer and the excavation height). The charts can be applied to estimate the exit gradient of the related case by multiplying the reduction factor by Eq. (4). Figure 3a illustrates the closer the distance between impermeable layer and the wall toe, the larger the decrease in the exit gradient value. Whereas, Fig. 3b shows that the increase of excavation height also reduces the magnitude of exit gradient. Those tendencies imply that a larger factor of safety against sand boiling can be attained by the decrease of the distance between wall toe and impermeable layer and the increment of the excavation height.

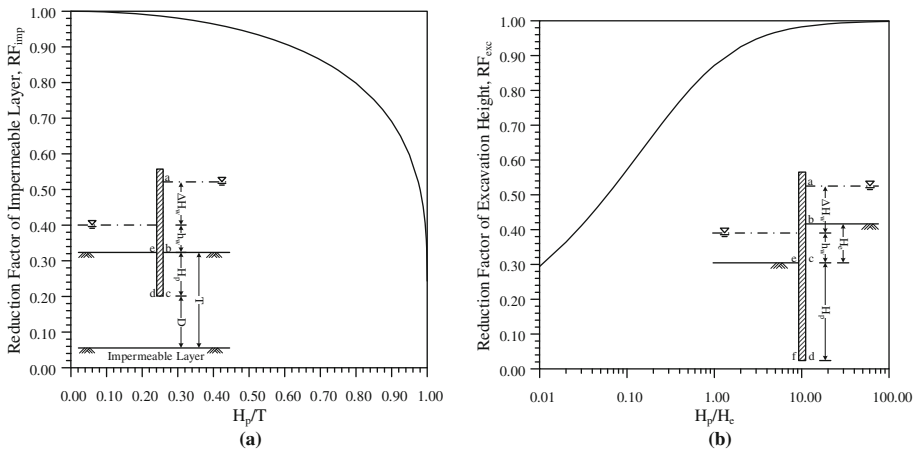


Fig. 3. Reduction factors of (a) the existence of impermeable layer and (b) the excavation height

Marsland (1953) conducted seepage model experiments on strutted excavations in either homogeneous coarse-grained soils or different soil strata to verify the results of the model test and those obtained mathematically. Figure 4 shows the Marsland (1953) factor of safety charts for various conditions. The factor of safety was estimated by taking an assumption that the groundwater level is at the same level as the ground level either at the downstream or upstream sides. The previous condition equals to heavy rainfall or flooding around the excavation. If the i_c value does not equal to one, the H_p/H_c component should be divided by i_c .

Ou (2006) suggested a simplified approach to estimating the factor of safety against sand boiling. By assuming the seepage flow is one-dimensional flow, and the hydraulic gradient is uniform along the flow path, the factor of safety equation is expressed as follows:

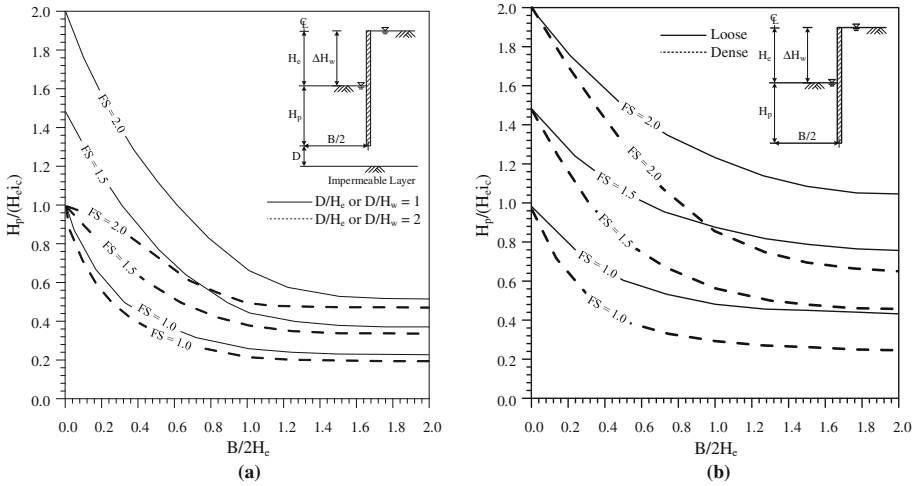


Fig. 4. Marsland (1953) factor of safety against sand boiling

$$FS = \frac{i_c}{i_{avg}} = \frac{\gamma'(H_e + 2H_p - d_i - d_j)}{\gamma_w \Delta H_w} \tag{5}$$

in which i_{avg} is the average hydraulic gradient along the flow path, H_e is the excavation height, and d_j stands for the distance between groundwater level and ground surface in the retained zone. According to Ou (2006), the factor of safety against sand boiling should be greater than or equal to 1.5.

After the overviews, it appears that the leading factor in designating the sand boiling failure due to seepage condition is the hydraulic gradient. Hydraulic gradient in groundwater flow case affects the magnitude of effective stresses acting on the soil particles. The movement of water inside the soil drags the soil particles in the direction of the current, and it produces additional forces. The upward flow as shown in Fig. 1 yields the decrease of the effective stress, whereas the downward flow will escalate the effective stress of the soil. Those manners imply the modification of the effective stress equation as shown in Eq. (6) for downward flow and Eq. (7) for upward flow.

$$\sigma'_v = \gamma_m z_1 + \gamma' x_1 + \gamma_w i_{down} x_1 \tag{6}$$

$$\sigma'_v = \gamma_m z_2 + \gamma' x_2 - \gamma_w i_{up} x_2 \tag{7}$$

in which σ'_v is the effective vertical stress of the soil, γ_m is the moist unit weight, γ' is the effective unit weight, z_i is the depth which is measured from the ground surface ($0 \leq z_1 \leq d_j$; $0 \leq z_2 \leq d_i$), x_i is the depth which is measured from the ground water level, i_{up} is the upward hydraulic gradient, and i_{down} is the downward hydraulic gradient. Consequently, the effective stress of soil and the hydraulic gradient are very fundamental in analysing the failure against seepage because they govern failure

mechanism of the soil. In the further analyses, it associates in controlling volume change and soil shear strength. Nonetheless, many features are still influencing the magnitude of hydraulic gradient in practice such as the geometry of cofferdam or excavation, the ratio of wall penetration to total soil thickness, wall behaviour, particle transport mechanism, and many other aspects.

3 Analysis Procedure

Marsland (1953) model tests in the homogeneous cohesionless soil were adopted in this study to investigate the failure mechanism of sand boiling and to observe the factor of safety value tendency in analysing failure case. The investigation involved numerical analysis using SEEP/W program and conventional methods of flow net to associate the results and to achieve a better understanding of the seepage failure mechanism. The cohesionless soil model is Ham River sand which is categorized into two different densities; relatively loose sand ($D_r = 59.35\%$) and dense sand ($D_r = 96.97\%$). The simulation consisted of 12 cases of homogeneous dense sand and 11 cases of

Table 1. Ham river sand parameter

Parameter	Unit	Loose sand	Dense sand	Reference(s)
Maximum void ratio, e_{max}		0.92		Bishop and Green (1965)
Minimum void ratio, e_{min}		0.59		Bishop and Green (1965)
Diameter at 60% passing, d_{60}	mm	0.25		Bishop and Green (1965)
Effective diameter, d_{10}	mm	0.16		Bishop and Green (1965)
Porosity, n		0.42	0.37	Marsland (1953)
Void ratio, e		0.72	0.59	
Relative density, D_r	%	59.35	96.97	
Critical hydraulic gradient, i_c		0.97	1.05	Marsland (1953)
Soil permeability, k	m/min	0.068	0.018	Chapuis (2004), Marsland (1953)
Saturated unit weight, γ_{sat}	kN/m ³	19.32	20.10	
Effective friction angle, ϕ'	degree	32.68	36.95	Kulhawy and Mayne (1990)
Effective Young's modulus, E	kPa	29221.59	37401.70	Seed and Idriss (1970)
Modulus of compressibility, m_v	1/kPa	3.42×10^{-5}	3.42×10^{-5}	

homogeneous loose sand under steady state flow type with the properties as shown in Table 1. The permeability of dense sand was estimated using Chapuis (2004) equation that is presented as follows:

$$k = 2.4622 \left[d_{10}^2 \frac{e^3}{1+e} \right]^{0.7825} \tag{8}$$

wherein k stands for soil permeability in cm/s, d_{10} is the effective diameter, and e is the void ratio. Even though the permeability of dense sand was evaluated using Chapuis (2004) equation, the permeability of loose sand was obtained directly from Marsland (1953) data. Moreover, for the reason that the material model under the isotropic homogeneous condition, the permeability of sand does not vary in any direction of flow and the magnitude is constant. Besides the soil parameter that is available in Marsland (1953), Bishop and Green (1965) in his study also provided some soil parameters of Ham River sand in which their values are also presented in Table 1.

Kulhawy and Mayne (1990) proposed a chart relationship between effective friction angle and the normalized dry unit weight of clean coarse-grained soils. Figure 5 depicts the friction angle of loose sand and dense sand in which the friction angle for loose sand in this simulation equals to 32.68° , and it equals to 36.95° for dense sand. With the purpose of estimating the modulus of compressibility of the Ham river sand, the following equation was used to determine the modulus of compressibility, m_v value:

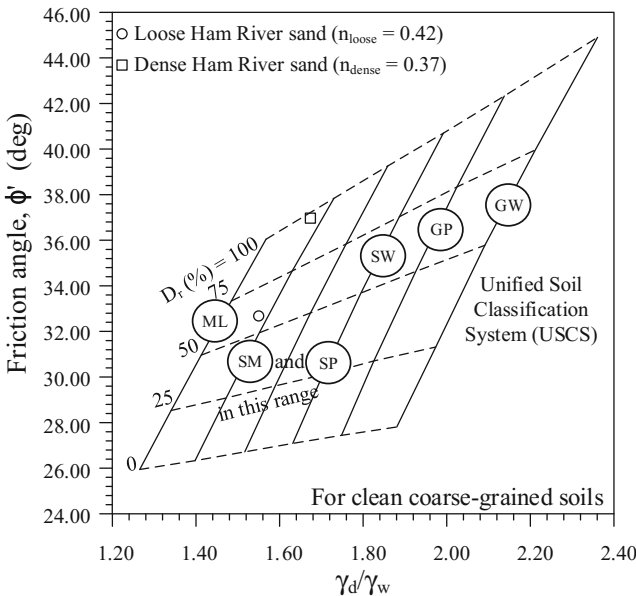


Fig. 5. Friction angle of Ham River sand

$$m_v = \frac{1}{E'} = \frac{1}{2G(1 + \nu')} \quad (9)$$

where E' stands for effective Young's modulus, G is the shear modulus, and ν' is the soil effective Poisson's ratio. The Poisson's ratio for this case equals to unloading/reloading Poisson's ratio, ν_{ur} which is equal to 0.20. The G value was predicted by using Seed and Idriss (1970) as shown in Eq. (10).

$$G = k_1 \sqrt{p'} \quad (10)$$

wherein the p' is the mean effective stress in MPa and the k_1 coefficient is a coefficient in a function of void ratio or relative density. The k_1 values in this simulation are equal to 344 and 445 for loose sand and dense sand, respectively.

The cofferdam models involve double-wall case and single wall case. The excavation width, B varies between 7.6 cm and 15.2 cm. Meanwhile, the B value equals to half of the seepage tank width which equivalents to 137.5 cm for the single-wall case. The wall penetration depth, H_p diverse from 2.5 cm to 15.2 cm whereas the wall toe was maintained at 7.6 cm above the impermeable boundary, D . The retained sand level was located at 38.0 cm above the wall toe. The wall structure is a brass plate with 0.125-inch thickness and attached to the brass spacers. The previous wall arrangement yields a relatively rigid retaining system with an unnoticeable wall deformation. Therefore, the wall movement is restrained either vertically or horizontally in the numerical simulation. The restriction of wall displacement in this simulation also leads to a simplification of the seepage problem and consistency against the conventional approaches. Moreover, the effect of the wall properties and the strutting system in this simulation will not affect the failure mechanism in the excavation zone. The details of the model tests and the experimental failure head difference, $\Delta H_{w,f}$ for loose sand and dense sand in accordance to Marsland (1953) are listed in Tables 2 and 3, respectively.

Table 2. Detail of model tests arrangement and experimental failure head of loose sand

Mnemonic name	D (cm)	B (cm)	H_p (cm)	H_e (cm)	$\Delta H_{w,f}$ (cm)
L0076025	7.60	7.60	2.50	33.50	7.75 ± 0.50
L0076051	7.60	7.60	5.10	30.90	11.60 ± 0.40
L0076076	7.60	7.60	7.60	28.40	14.50 ± 0.30
L0076102	7.60	7.60	10.20	25.80	17.00 ± 1.00
L0152025	7.60	15.20	2.50	33.50	9.50 ± 0.40
L0152051	7.60	15.20	5.10	30.90	15.30 ± 0.30
L0152076	7.60	15.20	7.60	28.40	19.10 ± 1.20
L0152102	7.60	15.20	10.20	25.80	20.00 ± 1.30
L1375025	7.60	137.50	2.50	33.50	11.30
L1375051	7.60	137.50	5.10	30.90	20.80
L1375076	7.60	137.50	7.60	28.40	29.00

Table 3. Detail of model tests arrangement and experimental failure head of dense sand

Mnemonic name	D (cm)	B (cm)	H _p (cm)	H _c (cm)	ΔH _{w,r} (cm)
D0076025	7.60	7.60	2.50	33.50	11.40 ± 0.40
D0076051	7.60	7.60	5.10	30.90	13.80 ± 0.30
D0076076	7.60	7.60	7.60	28.40	17.30 ± 0.30
D0076102	7.60	7.60	10.20	25.80	20.50 ± 0.40
D0076127	7.60	7.60	12.70	23.30	22.50 ± 0.40
D0076152	7.60	7.60	15.20	20.80	25.10 ± 0.20
D0152025	7.60	15.20	2.50	33.50	12.30 ± 0.80
D0152051	7.60	15.20	5.10	30.90	19.00 ± 0.50
D0152076	7.60	15.20	7.60	28.40	24.70 ± 0.50
D1375025	7.60	137.50	2.50	33.50	15.50 ± 0.20
D1375051	7.60	137.50	5.10	30.90	24.70 ± 0.40
D1375076	7.60	137.50	7.60	28.40	36.50 ± 0.50

The experimental failure head difference from Marsland (1953) corresponds to a failure criterion that a general movement of 0.2 mm observed in his experiment.

In addition to the discrepancy of excavation width and wall penetration depth in the numerical simulation, the various width of the prism of soil, S were also observed due to the upheave soil movement in the excavation zone as stated in Terzaghi (1943). In Terzaghi (1943), the excess hydrostatic pressure lifts the body of sand in a distance $H_p/2$, and as soon as it rises and deforms, the water-sand soil mixture starts to erupt. Although Terzaghi (1943) indicates a particular ground movement before failure, the deformation of the soil prism at failure is not the interest in this study. In this parametric study, the height of the prism was kept to the constant which equals to the wall penetration depth, H_p .

The aim of the width of the prism variation is to quantify the Terzaghi (1922) finding in the critical distance of the heave of the prism by examining the tendency of the factor of safety for different S/H_p ratio. There are six variations of the normalized S/H_p value which are 0.10, 0.20, 0.25, 0.33, 0.50, 0.67, and 1.00. Then, the hydraulic gradients inside the prism are arithmetically averaged, and the average value is denoted as i_{prism} . The factor of safety of each prism is estimated by Terzaghi (1922) factor of safety equation as shown in Eqs. (1) or (2). The parametric study allows exposing the most critical section at which the factor of safety exhibits the smallest magnitude of the factor of safety.

The observations were also carried out on the distribution of the effective stresses and the normalized hydraulic gradient (i_e/i) contours in the excavation zone, and also on the tendency of the factor of safety value from several methods. The magnitudes of the factor of safety against piping that was evaluated using various approaches were plotted together to conclude the test condition; failure or not failure. When the effective stress value is zero or negative, and the Terzaghi (1922) or Harza (1935) factor of safety value is less than or equal to one, the soil is defined as the failure state.

4 Results and Discussions

The results of the parametric study on the variation of the width of the prism are illustrated in Fig. 6. It shows the common trend line of the Terzaghi (1922) factor of safety against the width of the prism in both loose sand and dense sand is started by a high magnitude of the factor of safety near the sheet pile; then it continuously decreases until it reaches the inflection point. The inflection point is a point at which the trend of the factor of safety change the slope, and it also indicates the lowermost value of the factor of safety. It can be seen in Fig. 6 that the inflection point in loose sand is located at a distance from the wall equals to $H_p/3$, while in the dense sand it equals to $H_p/4$. The smallest factor of safety for each model falls in the range of $H_p/4$ to $H_p/2$ for loose sand and $H_p/5$ to $H_p/3$ for dense sand. This finding indicates the critical prism that its width is within the range is susceptible to piping failure due to heave, and at the same time the prism has a higher probability to rise or deform. In addition to the determination of the critical width, the width of the critical prism is also sensitive to the of excavation geometry, especially to the excavation width, B. The increase of B value changes the critical width of the soil prism, $S_{critical}$ into a narrower size and becomes closer to the wall. This tendency can be observed in both loose sand and dense sand cases. Consequently, in an attempt to generalize the critical section of the prism, the width of the soil prism equals to $H_p/3$ can be considered adequate to represent the most critical dimension of the prism.

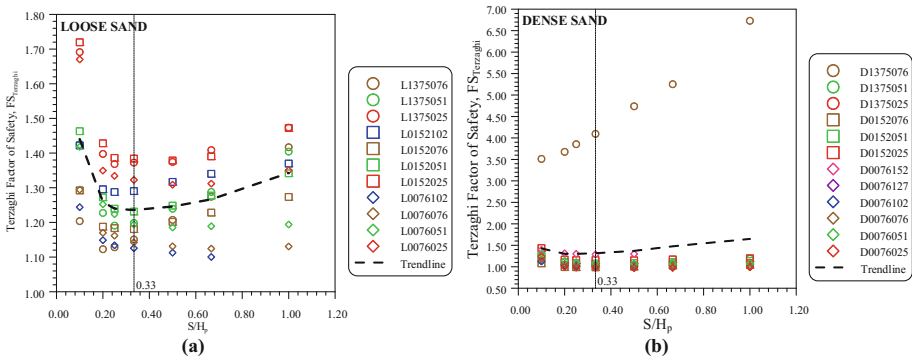


Fig. 6. Terzaghi factor of safety for a various width of the soil prism in (a) loose sand and (b) dense sand

Figure 7 shows the analysis results of the factor of safety magnitude against sand boiling using various methods. The study was carried out by using five approaches; Terzaghi (1922), Harza (1935), Marsland (1953), Harr (1962), and the simplified one-dimensional method of Ou (2006). The Terzaghi (1922) method in this part is assumed that the prism has a width equals to $H_p/2$ as postulated by Terzaghi (1922). Afterward, the hydraulic gradient of the submerged prism within the distance of $H_p/2$ is averaged. Meanwhile, the exit gradient, i_e for the Harza (1935) equation was directly

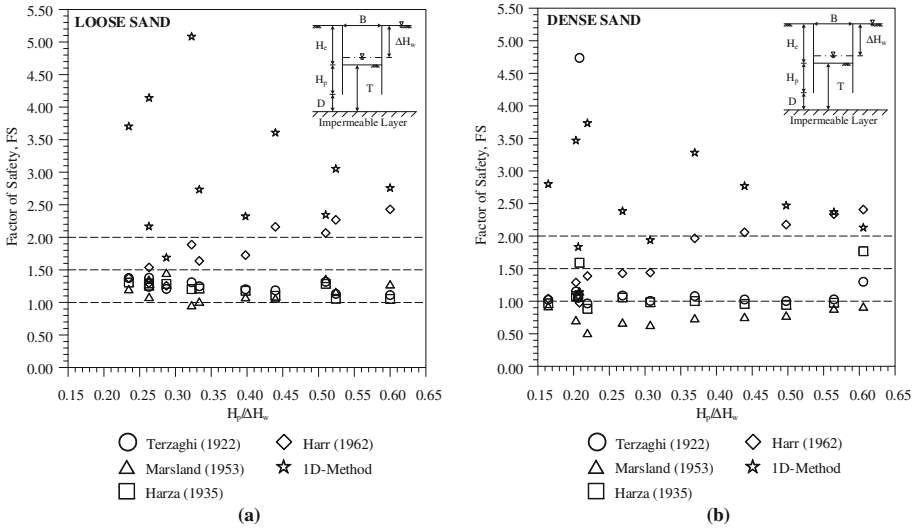


Fig. 7. Factor of safety magnitude in (a) loose sand and (b) dense sand

obtained from SEEP/W program output at the location near the wall. Figures 2a and 4a were used to estimate the factor of safety against sand boiling in accordance to Harr (1962), and Marsland (1953) approaches, respectively. The results exhibit the overall range of the factor of safety value for Marsland (1953) model tests in loose sand ranges from 0.96 to 5.08, whereas the factor safety ranges from 0.51 to 4.74 in dense sand model tests. The common trend in this analysis is the factor of safety values from Terzaghi (1922), Harza (1935), and Marsland (1953) methodologies are close to each other. Specifically, the Terzaghi (1922) and Harza (1935) methods appear to have a close magnitude of the factor of safety in both loose sand and dense sand. The typical value of the factor of safety in loose sand and dense sand based on Terzaghi (1922), Harza (1935), and Marsland (1953) methods are successively 1.21 and 1.10. These results also not only show that the Terzaghi (1922), Harza (1935), and Marsland (1953) techniques correspond to the failure test condition can describe the original circumstances of the test, but also Marsland cases might not be the total failure condition. Although it does not represent the complete failure condition where the flow of soil particles is noticeable, Marsland (1953) did a rigorous observation on the head difference at the onset of the excavation surface deformation.

In contrast to those methods, the simplified one-dimensional (1D-Method) and Harr (1962) methods seem to overestimate the factor of safety magnitude in this case. The average factor of safety from the simplified one-dimensional method is 2.53 for dense sand and 3.05 for loose sand. Whereas, the factor of safety magnitudes are 1.63 and 1.79 for Harr (1962) method in dense sand and loose sand cases, respectively. In addition to the obtained value of the factor of safety, both equations, the Harr (1962) and the simplified one-dimensional methods exhibit a different trend. Harr (1962) has a

tendency that the factor of safety increases along with the rise of $H_p/\Delta H_w$ ratio, whereas the trend of 1D-Method goes down in consort with the escalation of $H_p/\Delta H_w$ ratio. That behaviour can be observed in both loose sand and dense sand. Both trends show an unreasoned tendency because the cases that were used in this study are the failure cases. Theoretically, the factor of safety should be close to one or less than one due to the failure condition.

The previous behaviour can be explained by the assumptions that are used in the equation about the geometry of excavation and the soil condition. Both Harr (1962) and 1D-Method assume the excavation width, B and the depth of impermeable layer, T are infinite. In fact, the excavation model has an absolute value of excavation width, B and a certain depth of impermeable layer, T . The change in T and B values will not alter the magnitude of the factor of safety by those methods. On the contrary, those factors affect the extent of the hydraulic gradient in which it also affects the factor of safety. Subsequently, the assumption of the simplified one-dimensional technique that the flow path is measured from the upstream groundwater level to the downstream groundwater level may lead to a relatively high value of the factor of safety because of a relatively long flow path that decreases the magnitude of hydraulic gradient. Although, the effect of the excavation geometry and the depth of impermeable layer are the factors that have to be more reckoned with in the analysis of seepage.

The failure mechanism of an excavation corresponds to groundwater flow is not only determined by the ratio of the hydraulic gradient to critical hydraulic gradient but also can be expressed by the value of effective stress. Figures 8, 9 and 10 show the normalized gradient of i_c/i , effective stress, and total pore water pressure contours for L0076076, D0076076, L0152076, and D0152076 cases successively. The normalized gradient and effective stress contours in Figs. 8 and 9, respectively represent similar patterns in term of the critical zone at which the i_c/i ratio is equal or smaller than one, and the effective stress is equal or smaller than zero. The crucial area for all cases is located near the wall toe. Similar patterns are also observed in the different model case. It explains that the region at which the i_c/i ratio is less than or equal to one, the corresponding effective stress will be equal or smaller than zero. At the same time, the related region will experience significant shear strain due to loss of soil shear strength. Furthermore, the total pore water pressure distributions in Fig. 10 indicates that the highest pore water pressure occurs at the toe of the wall. Nonetheless, the pore water pressure distributions along the excavation width, B are not uniform. The total pore water pressure at the section of $B/2$ is smaller than that is located near the wall toe.

Figures 8 and 9 illustrate the failure shape always corresponds to a relatively rectangular soil prism. Nevertheless, the width of the prism does not equal to the Terzaghi (1943) suggestion. According to the i_c/i and effective stress contours, the critical zone in the case of dense sand covers a larger region than in the loose sand. The critical area in the loose sand cases usually localized near the wall toe except for a narrow excavation where the wall penetration is larger than or equal to excavation width. Conversely, the effective stress zone that the value equals to zero in the case of dense sand and narrow excavation cases equally distributes near the excavation surface to the wall toe. In the case of narrow excavation, both loose sand and dense sand

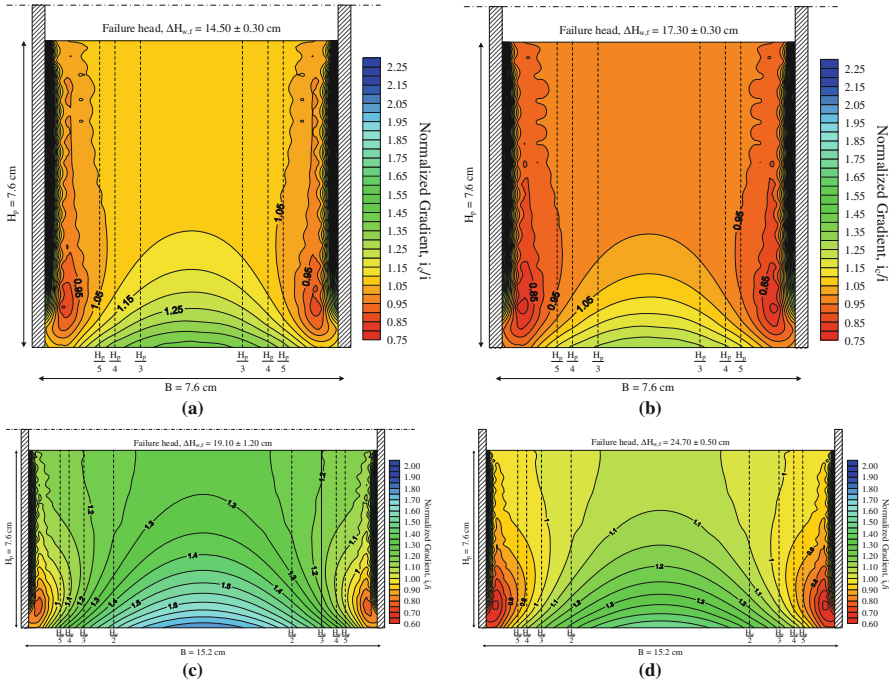


Fig. 8. Normalize gradient, i_c/i contour of (a) L0076076, (b) D0076076, (c) L0152076, and (d) D0152076 cases

exhibit the similar pattern of critical effective stress distribution. The examination of these findings indicates that the most likely possible failure type is the heave of the soil prism for loose sand cases and local failure which is marked the expulsion of the soil-water mixture for dense sand and narrow excavation cases. The concentrated area in the loose sand cases at which the effective stress value is equal or smaller than zero, the pore water pressure acts on the soil body that does not fail. As soon as the pore water pressure exceeds the weight of the soil, the soil will start to deform, and sand boiling occurs. Meanwhile, the zero effective stress in the dense sand and narrow excavation cases that are located near the excavation surface and along the wall penetration depth produces no resistance against the pore water pressure, and it is followed by the expulsion of the groundwater together with transported soil particles to the excavation surface. As a result, the sand boiling occurrence is inevitable.

Referring to Terzaghi (1943) that he explained the general mechanism of piping failure due to heave is caused by the difference of the water head between upstream and downstream that induces water flows near the retaining wall through the soil particles. The groundwater flow in excavation zone contributes to the decrease of the effective stress of the soil. As the effective stress decreases in the excavation area, the soil gradually loses its strength and at a particular condition at which the effective stress is

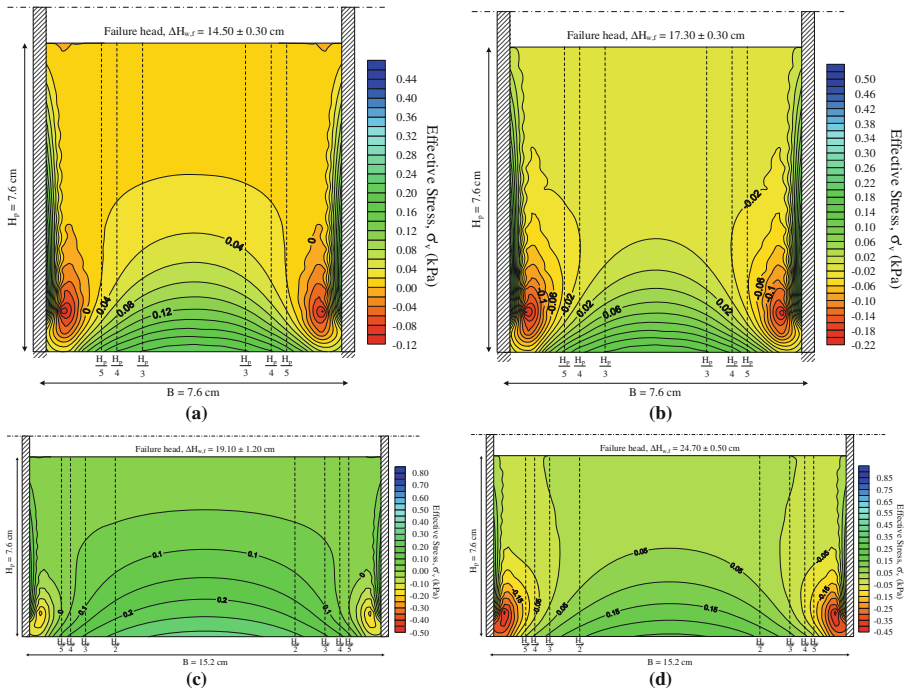


Fig. 9. Effective stress contour of (a) L0076076, (b) D0076076, (c) L0152076, and (d) D0152076 cases

equal to zero the soil cannot sustain any stresses. The soil becomes loose at the downstream side wherein the void ratio, e , porosity, n , and the permeability, k of the soil also escalate. At that condition, the soil prism starts to rise, and sand boiling failure occurrence follows it. A similar mechanism of sand boiling failure in the excavation zone was also observed by Tanaka et al. (2016). Concerning Marsland (1953) experiment results, he explained that the failure in the homogenous loose sand occurs when the amount of excess hydrostatic pressure is sufficient to encounter the submerged weight of the soil prism. Whereas, the failure in the homogeneous dense sand took place when the ratio between i_c and i_e equal to one. Therefore, the presumption using effective stress distribution and a proportion of the hydraulic gradient can be reasonable to describe and predict the failure mechanism against sand boiling failure. Even though the deformation of the excavation surface cannot be captured by this method, observation based on the effective stress distribution in the excavation area is highly suggested to be performed to forecast the critical section and the failure mechanism against sand boiling.

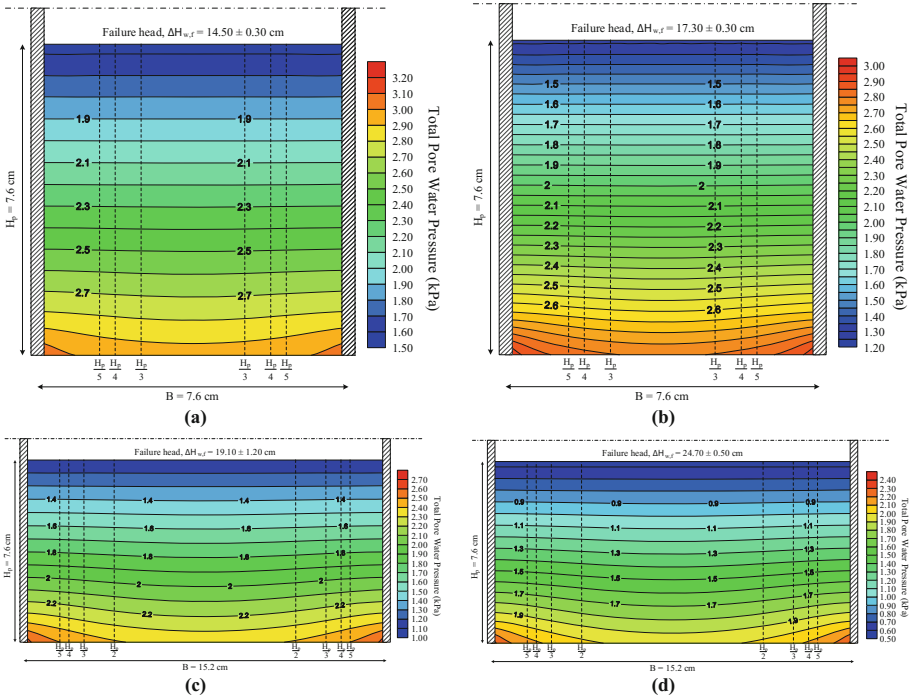


Fig. 10. Total pore water pressure distribution of (a) L0076076, (b) D0076076, (c) L0152076, and (d) D0152076 cases

5 Conclusion

The understanding of the factors affecting sand boiling failure is necessary to estimate the safety of an excavation in cohesionless soil under high groundwater level condition and to predict the failure mechanism. A series of parametric study on the experimental failure case and numerical analysis were carried out by using numerical programs and conventional methods. The observation of the analysis results was focused on the factor of safety magnitude from various methods, hydraulic gradient, and effective stress distribution in the excavation zone. According to the outcomes, the conclusions of this study are shown as follows:

1. By considering the effect of excavation geometry and the existence of impermeable soil layer in the Marsland (1953) case, a distance of $H_p/3$ from the wall with a height equals to H_p can be considered adequate to represent the most critical prism section of which it has the lowermost magnitude of the factor of safety.
2. Terzaghi (1922) and Harza (1935) approaches are consistent with each other and can simulate the closest failure condition of the Marsland (1953) experimental failure model. Nonetheless, Marsland (1953) experimental failure models are not the complete failure model where the discharge of soil-water mixture is observable.

3. In addition to the computation of factor of safety of excavation, observation on the effective stress distribution is highly recommended to be conveyed to predict the critical area and the failure mechanism of sand boiling.
4. According to the previous findings on the i_c/i contours and the effective stress distributions, the most likely possible failure mechanism of loose sand is a piping failure due to heave. Meanwhile, for the dense sand and narrow excavation cases, the failure mechanism is exhibited by the expulsion of the sand-water mixture on the excavation surface.

References

- Bishop, A.W., Green, G.E.: The influence of end restraint on the compression strength of a cohesionless soil. *Geotechnique* **15**(3), 243–266 (1965)
- Chapuis, R.P.: Predicting the saturated hydraulic conductivity of sand and gravel using effective diameter and void ratio. *Can. Geotech. J.* **41**(5), 787–795 (2004)
- Harr, M.E.: *Groundwater and Seepage*, pp. 104–125. McGraw-Hill, New York (1962)
- Harza, L.F.: Uplift and seepage under dams on sand. *Trans. Am. Soc. Civ. Eng.* **100**(1), 1352–1385 (1935)
- Kulhawy, F.H., Mayne, P.W.: *Manual on Estimating Soil Properties for Foundation Design*. EPRI Report EL-6800, Research Project 1493-6, Cornell University, NY (1990)
- Marsland, A.: Model experiments to study the influence of seepage on the stability of a sheeted excavation in sand. *Geotechnique* **3**(6), 223–241 (1953)
- Seed, H.B., Idriss, I.M.: *Soil Moduli and Damping Factors for Dynamic Response Analyses*. Report EERC 70-10, Earthquake Engineering Research Center, University of California, Berkeley (1970)
- Tanaka, T., Tachimura, R., Kusumi, S., Nagai, S., Inoue, K.: Experimental findings of 3D seepage failure of soil within a cofferdam. *Jap. Geotech. Soc. Spec. Publ.* **2**(45), 1608–1613 (2016)
- Terzaghi, K.: Der grundbruch on stauwerken und seine verhutung. *Die Wasserkraft* **17**(24), 445–449 (1922). (in Germany)
- Terzaghi, K.: *Theoretical Soil Mechanics*, pp. 257–262. Wiley, New York (1943)
- Ou, C.Y.: *Deep Excavation: Theory and Practice*, pp. 163–167. Taylor & Francis Group, London (2006)